


RESEARCH ARTICLE

Thoracic vertebral morphology in normal and scoliosis deformity in skeletally immature rabbits: A Longitudinal study

Ausilah Alfraihat¹  | John Casey Olson² | Brian D. Snyder³ | Patrick J. Cahill⁴ | Sriram Balasubramanian¹

¹School of Biomedical Engineering, Science and Health Systems, Drexel University, Philadelphia, Pennsylvania

²Beth Israel Deaconess Medical Center, Boston, Massachusetts

³Harvard Medical School, Boston, Massachusetts

⁴Children's Hospital of Philadelphia, Philadelphia, Pennsylvania

Correspondence

Sriram Balasubramanian, School of Biomedical Engineering, Science and Health Systems, Drexel University, Philadelphia, PA.
Email: sb939@drexel.edu

Abstract

Objective: To measure age-related changes in thoracic vertebral body heights (VBH) in skeletally immature normative and scoliotic rabbits to assess how VBH change during growth. To examine the potential link between the moment-arm of the rib tether and vertebral wedging as well as the sum of the curvature angles at the apical level (T7). To assess the correlation between the magnitude of initial spine curve and final spine curve in the scoliotic group.

Methods: Eight healthy, skeletally immature normative New Zealand rabbits and ten skeletally immature scoliotic rabbits which underwent unilateral rib tethering were included retrospectively. Each rabbit was scanned at two to four time points (at 7, 11, 14 and 28 weeks). Three dimensional bone models of thoracic vertebrae (T1-T12) were digitally segmented and reconstructed. VBH were calculated using surface landmark points from each thoracic vertebra. Apical level (T7) \pm 2 levels in scoliotic rabbits were compared to their corresponding levels and time points in the normative group. The moment-arms between the centroids of 2D projections of T3-T9 vertebral bodies and the line which connects the centroids of the end levels were calculated.

Results: Bilateral left-right (L-R) symmetry and anterior-posterior (A-P) asymmetry were observed in normative VBH. Bilateral concave-convex (CC-CX) asymmetry and (A-P) asymmetry were observed in scoliotic VBH. No significant differences in growth rates were found between the normative and scoliotic groups. Vertebral wedging as well as curvature magnitude were positively correlated with the moment-arms.

Conclusion: Unilateral rib tether applies compressive forces on both concave and convex sides, whereas compressive forces are lower on the latter. Knowing the

This is an open access article under the terms of the Creative Commons Attribution-NonCommercial-NoDerivs License, which permits use and distribution in any medium, provided the original work is properly cited, the use is non-commercial and no modifications or adaptations are made.

© 2020 The Authors. *JOR Spine* published by Wiley Periodicals LLC on behalf of Orthopaedic Research Society.

amount of vertebral wedging or curve magnitude would enable us to predict the applied force (moment-arms), which is important for planning a corrective surgery.

KEYWORDS

asymmetric loading, cobb angle, kyphosis angle, moment-arms, scoliosis, unilateral rib tethering, vertebral body heights, vertebral wedging

1 | INTRODUCTION

Scoliosis is a common disorder of the spine that results in three dimensional (3D) deformity.¹ According to the National Scoliosis Foundation, the incidence of scoliosis ranges between 2% and 3% among the general population.² A subset of these patients (1 to 2 per 10 000 births) present at an age at which the majority of musculoskeletal growth has yet to occur.² Early-onset scoliosis (EOS) represents a group of congenital and acquired conditions that affect the growth and development of the spine and thorax in children. Scoliosis progression in skeletally immature EOS patients depends on the remaining growth of the spine. Abnormal growth of the spinal column involves increasing asymmetries in vertebral body and intervertebral disc (IVD) morphologies,^{3,4} that directly affects the volume, symmetry, and function of the thorax, and indirectly affects lung growth and function. These alterations in normal growth of the spine also affect the mechanics of the spine as well as the vertebral growth plates.

Previous studies have theorized about the biomechanical role of asymmetrical loading in progression of scoliotic deformity.⁵⁻⁷ An asymmetric load leads to asymmetrical longitudinal growth and hence wedging of the vertebral bodies and IVDs in a vicious cycle.⁸ Nonoperative treatments such as bracing are designed to counteract these asymmetric loads.^{9,10} Currently, surgery is recommended for EOS patients with Thoracic Insufficiency Syndrome (TIS) that is characterized by reduced lung growth and function as a result of a progressive spine deformity. The treatment of scoliosis in children is evolving - the previous approach of correcting the spine by instrumenting multiple levels and fusing the spine early has been shown to inhibit growth and development of the lungs and decrease pulmonary function.^{11,12} Newer growth friendly deformity correction methods such as growing rods and vertebral tethers modulate vertebral growth while allowing continued thoracic growth. Spine growth modulation for scoliosis correction is a technique for slowing growth on the convex side of the curve and enhancing growth on the concave side by the application of Hueter-Volkman principle of mechanotransduction; this application results in gradual deformity correction.¹³ Hueter-Volkman principle states that mechanical factors influence longitudinal bone growth and remodeling, wherein compressive forces inhibit growth and tensile forces stimulate growth. Growth friendly techniques are less invasive than traditional spine fusion.¹³ While several retrospective studies have shown improvement in curve magnitude using growth friendly techniques; apparent cases of overcorrection or undercorrection of scoliosis have also been reported.¹³⁻¹⁵

To overcome such complications, before these devices can be implemented reliably for the treatment of scoliosis, it is necessary to understand longitudinal growth patterns of the normative spine, and study any alterations in these growth patterns with scoliosis. Several animal studies have reported relationships between vertebral growth, growth rates, and mechanical stresses in long bones and caudal vertebrae. Long bone and vertebral growth were reported to decelerate under compression, and accelerate by a smaller amount under distraction.^{16,17} Studies on growth plates have reported the proportional alteration in growth rate of caudal vertebrae and proximal tibiae growth plates of three different species (rat, rabbit, and calf) in response to differing magnitudes of stress.¹⁸ Furthermore, for both caudal vertebrae and proximal tibia, the growth sensitivity to stress (percent change per unit stress) did not differ by species and age of animal, but varied with anatomical location where it was significantly greater in tibiae than vertebrae. Previous studies have not reported the effect of growth modulation on spine vertebrae which are different than the non-weight bearing caudal (tail) vertebrae. Hence, the current study aims to investigate the growth patterns of thoracic spine vertebral bodies between skeletally immature normal and scoliotic rabbits. It is noteworthy that direction of loading in human spine is different than the loading in the spine of quadrupeds. The loading in the human spine is in axial and posterior direction, whereas in quadrupeds the spine is loaded in axial and anterior direction. Furthermore, quadruped spines are subjected to greater axial compressive loading as compared to the upright human spine. As a result, the bone density of the vertebral bodies in quadrupeds are two to four times greater than those in humans.^{19,20} However, it has been observed that the trabeculae of the vertebral bodies of both biped and quadruped spines are oriented from endplate to endplate indicating that they both undergo loading in the axial direction.²¹

The objectives of the current study are to: a) measure and compare age-related changes in thoracic vertebral body heights (VBH) in skeletally immature normative and scoliotic rabbits, b) correlate moment-arm of the rib tether with vertebral wedging as well as the sum of curvature angles at the apical level (T7), and c) correlate the magnitude of initial spine curve and the final spine curve in the scoliotic group. We hypothesize that: a) VBH growth patterns will be different between normative and scoliotic rabbits, and that there will be age-related bilateral and anterior-posterior (A-P) differences in the scoliotic group, b) moment-arm of the rib tether will positively correlate with vertebral wedging as well as the sum of the curvature angles at the apical level (T7), and c) greater initial curve magnitude would result in greater final curve magnitude.

2 | METHODS

2.1 | Animal details

Chest computed tomography (CT) scans were obtained retrospectively from a total of 18 female skeletally immature New Zealand rabbits (Normal: $n = 8$, average weight: 2.87 ± 1.035 kg; Scoliotic: $n = 10$, average weight: 2.76 ± 1.019 kg). Based on somatic growth of rabbits compared to humans, a three week old rabbit is equivalent to a three year old child, while a 28 week old rabbit is considered equivalent to a full grown adult.²² For the scoliotic group, rabbits were received at the age of four weeks and were tethered 5, 6 or 7 days after arrival (Table 2). All animal procedures were approved and monitored by the Beth Israel Deaconess Medical Center (BIDMC) institutional animal care and use committee. Rabbits underwent unilateral rib tethering surgery. A rib tether was attached to rib two or three and rib eight or nine, comprising the right hemithorax (Figure 1) to create a progressive, left convex, scoliosis deformity.^{22,23} Additional details about the surgery can be found in a previously published work.^{22,23} Each rabbit was scanned at 2 to 4 time points (i.e., at approximately 7, 11, 14, and 28 weeks after birth). The rabbits were positioned prone on a Toshiba Aquilion 64 scanner with resolution of $0.26 \text{ mm} \times 0.26 \text{ mm}$ in the transverse plane, and 0.3 mm slice spacing.²³ Details of the animals used in this study are shown in Table 1, and scoliotic rabbits demographics and radiographic data are shown in Table 2.

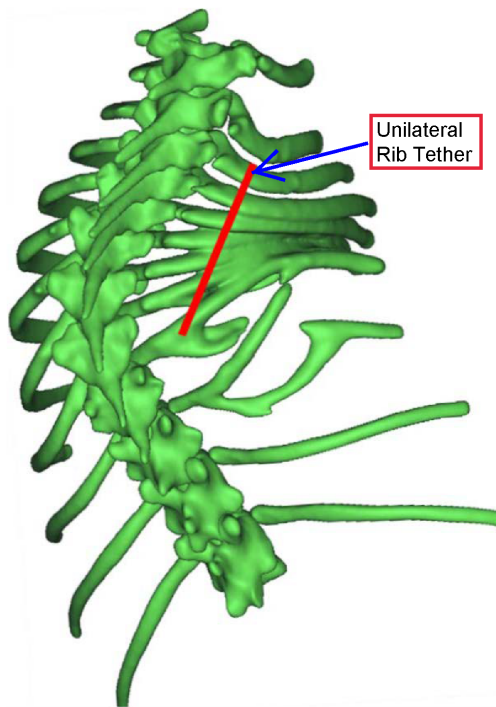


FIGURE 1 3D reconstruction of rabbit chest CT scan with virtual rib tether placed on the right ribs at T3 and T9

TABLE 1 Details of the normal and scoliotic rabbits used in this study

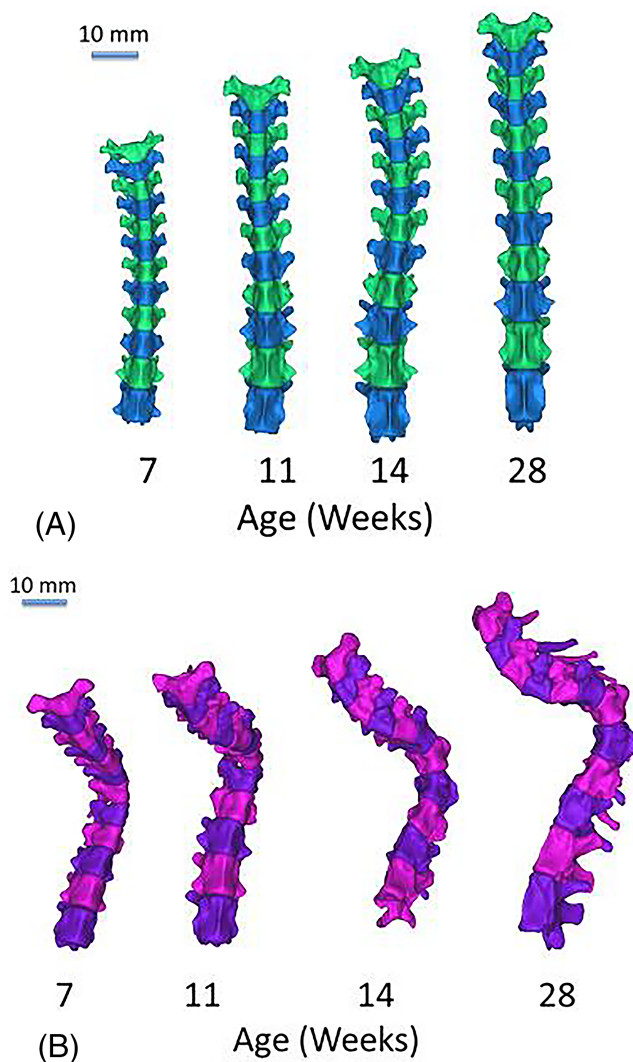
| | Normal | Scoliotic |
|---------------------------------------------------------------------------------------------------|------------------|-------------------|
| Number of animals scanned at first time point: 7 weeks | 5 | 8 |
| Number of animals scanned at second time point: 11 weeks | 6 | 10 |
| Number of animals scanned at third time point: 14 weeks | 8 | 10 |
| Number of animals scanned at fourth time point: 28 weeks | 8 | 10 |
| Age (Mean \pm SD) at first time point (weeks) | 6.47 ± 0.57 | 7.62 ± 0.58 |
| Age (Mean \pm SD) at second time point (weeks) | 10.87 ± 0.69 | 10.57 ± 0.53 |
| Age (Mean \pm SD) at third time point (weeks) | 14.88 ± 0.82 | 15.10 ± 0.83 |
| Age (Mean \pm SD) at fourth time point (weeks) | 27.90 ± 0.44 | 26.52 ± 3.40 |
| Cobb angle (Mean \pm SD) of (T3-T9) at first time point ($^{\circ}$) | - | 34.04 ± 12.66 |
| Cobb angle (Mean \pm SD) of (T3-T9) at second time point ($^{\circ}$) | - | 43.4 ± 21.98 |
| Cobb angle (Mean \pm SD) of (T3-T9) at third time point ($^{\circ}$) | - | 44.3 ± 16.53 |
| Cobb angle (Mean \pm SD) of (T3-T9) at fourth time point ($^{\circ}$) | - | 47.4 ± 17.39 |
| Cobb angle increase (Mean \pm SD) between first time point and second time point ($^{\circ}$) | - | 9.36 ± 12.77 |
| Cobb angle increase (Mean \pm SD) between second time point and third time point ($^{\circ}$) | - | 0.9 ± 13.21 |
| Cobb angle increase (Mean \pm SD) between third time point and fourth time point ($^{\circ}$) | - | 3.1 ± 9.67 |
| Duration (Mean \pm SD) between first time point and second time point (weeks) | 4.2 ± 1.12 | 2.82 ± 0.99 |
| Duration (Mean \pm SD) between second time point and third time point (weeks) | 3.93 ± 0.44 | 4.48 ± 0.44 |
| Duration (Mean \pm SD) between third time point and fourth time point (weeks) | 13.02 ± 0.83 | 11.74 ± 2.94 |

2.2 | 3D reconstruction and measurement of vertebral body heights

Thoracic vertebrae (T1-T12) were digitally segmented and reconstructed using the medical image processing software MIMICS (Materialize Inc., Belgium) at a preset threshold for bone (Figure 2A,B). 3D surface landmark points (Figure 3) were identified for each vertebra using a custom script (MATLAB, Mathworks Inc, Natick,

TABLE 2 Scoliotic rabbits demographics and radiographic data

| Rabbit# | Tethering time after arrival (days) | First rib tethered | Distance from spinous process (mm) | Last rib tethered | Distance from spinous process (mm) | Apex |
|---------|-------------------------------------|--------------------|------------------------------------|-------------------|------------------------------------|------|
| 14-1 | 6 | 3 | 27.16 | 9 | 28.46 | T7 |
| 15-1 | 6 | 3 | 24.51 | 8 | 33.13 | T6 |
| 19-1 | 7 | 3 | 29.04 | 9 | 21.45 | T7 |
| 23-1 | 5 | 3 | 27.81 | 9 | 30.23 | T7 |
| 25-1 | 5 | 2 | 26.23 | 8 | 29.35 | T6 |
| 26-1 | 5 | 3 | 27.47 | 9 | 32.3 | T7 |
| 27-1 | 6 | 3 | 24.92 | 9 | 31.44 | T6 |
| 28-1 | 6 | 3 | 28.31 | 9 | 34.65 | T7 |
| 24-2 | 6 | 3 | 23.61 | 9 | 35.69 | T7 |
| 25-2 | 6 | 3 | 25.73 | 9 | 36.33 | T7 |

**FIGURE 2** Surface geometry reconstructions of T1-T12 vertebrae from manually segmented chest CT scans using MIMICS at four time points. (A) Exemplar normative rabbit #30 and (B) Exemplar scoliotic rabbit #19-1. CT, computed tomography

Massachusetts). The method of bony landmark identification was based on Peters et al.²⁴⁻²⁶ The identified landmark points of each vertebra were used to measure vertebral body heights (VBH) (Right, left, anterior and posterior). In this paper VB_L^H and VB_R^H refer to left and right VBH in the normative group, respectively. Whereas VB_{CX}^H and VB_{CC}^H refer to left (convex) and right (concave) VBH in scoliotic group, respectively. VB_P^H and VB_A^H refer to posterior and anterior VBH in both normative and scoliotic groups. The apical level was considered to be T7, as the majority of rabbits had T7 as the apex. The apical level (T7) and adjacent upper (T5,T6) and lower (T8,T9) vertebrae (i.e., apical level ± 2 levels) from the scoliotic group were compared to their corresponding levels and time points in the normative group.

2.3 | Statistical analysis

Based on the normality of the data determined by Shapiro-Wilk test, parametric tests were performed for statistical analysis. All statistics were calculated using SPSS 20.0.0 software (IBM Inc., Armonk, New York) with a significance level of $p < 0.05$.

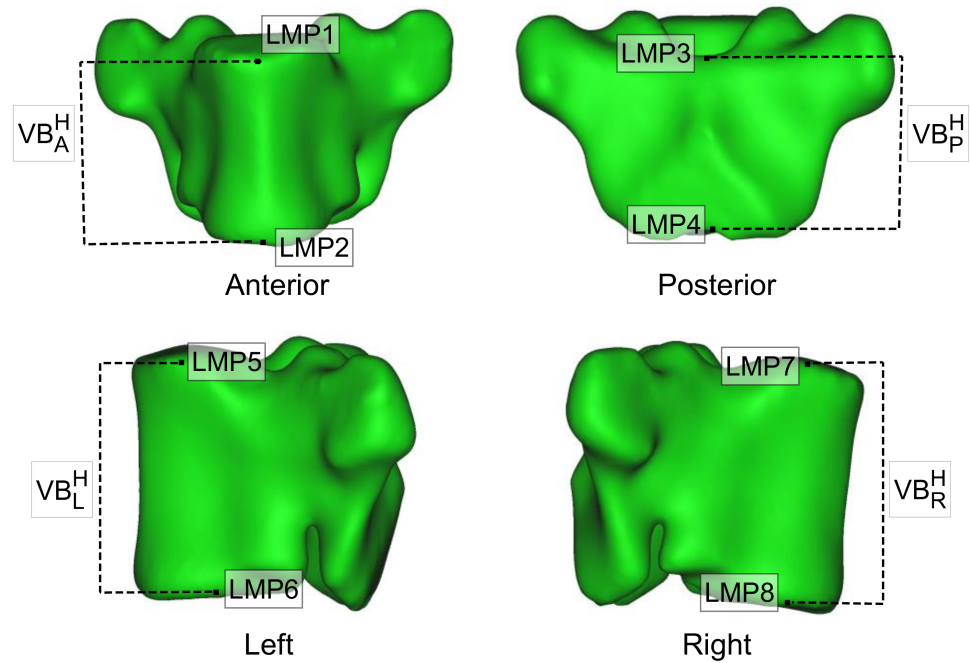
2.3.1 | Bilateral (left-right) and Anterior-Posterior symmetry

Paired sample t-tests were used to assess bilateral (right-left) and anterior-posterior (A-P) symmetry within each group.

2.3.2 | Vertebral wedging

Vertebral wedge deformity in the coronal and sagittal planes were calculated as the ratio of the left to right vertebral body heights (VB_L^H / VB_R^H), (VB_{CX}^H / VB_{CC}^H), and ratio of the posterior to anterior vertebral body heights (VB_P^H / VB_A^H), respectively. A value of one would be indicative of geometric symmetry.

FIGURE 3 Vertebral body landmark points (LMPs) used for measuring vertebral body heights



2.3.3 | Growth rates

For all animals, growth rates were calculated for each vertebral measurement at each vertebral level. Linear regression models (as shown in Equation 1) were used to estimate the growth rates (i.e., slope of the linear regression model) for each measurement for the entire age range. The growth rates of normal and scoliotic groups at corresponding levels and time points compared using independent sample *t*-test.

$$\text{Geometric measure} = b_1 * (\text{age in days}) + b_0 \quad (1)$$

where b_0 is the value of the geometric measure at birth, and b_1 is the rate of change of the geometric measure with age (i.e., growth rate).

2.4 | Moment-arm of rib tether

For each 3D reconstruction in the scoliotic group, MIMICS (Materialise Inc., Belgium) was used to export the vertebral body of each vertebrae T3-T9 as a 3D point cloud. 3D point clouds exported (in mm) from MIMICS have the coronal view in the X-Z plane and the sagittal view in the Y-Z plane. Using MATLAB (Mathworks Inc, Natick, MA), 2D projections of the 3D point clouds of the vertebral bodies were performed. The 2D projection of each point $p = (X,Y,Z)$ onto the X-Z plane is the point $p = (X,0,Z)$ (Figure 4A) and in the Y-Z plane is the point $p = (0,Y,Z)$ (Figure 4B). Contours of the T3 to T9 vertebral bodies were derived from their 2D projections. Then the centroid of each contour was calculated and plotted. Using the centroids of the end vertebrae T3 and T9 (namely A and B, respectively), the equation of the straight line joining those two points (denoted as AB) was calculated and the line was plotted (Figure 4C). The moment-arms (i.e.,

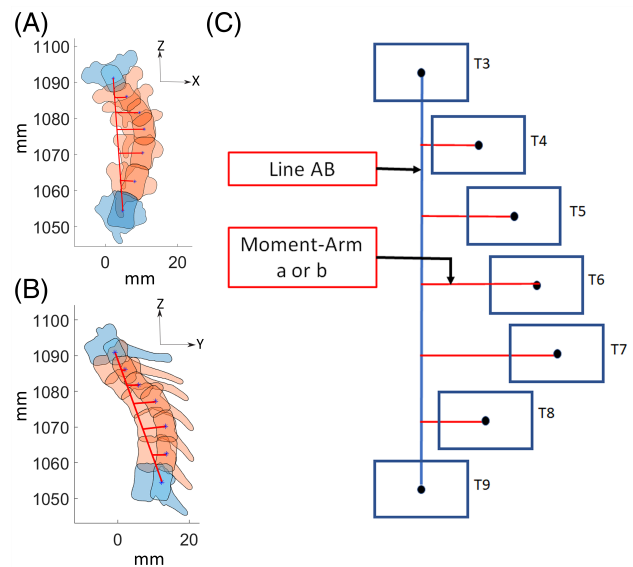


FIGURE 4 (A) 2D projection of vertebral bodies in the frontal plane, (B) 2D projection of vertebral bodies in the sagittal plane, (C) Schematic of the 2D projection of the vertebral bodies and the moment-arm (a in the frontal plane, b in the sagittal plane) calculated between the centroids of the vertebral bodies and the line AB. 3D, three dimensional

shortest distance) between the centroids of each contour T4-T8 and line AB were calculated in the frontal plane (denoted as a) and in the sagittal plane (denoted as b), respectively. The magnitude of the initial spine curvature (i.e. Cobb angle) is related to the initial force applied by the rib tether. However, since the rib tether force was not measured, the moment-arm of the rib tether could serve as a surrogate for the applied force.

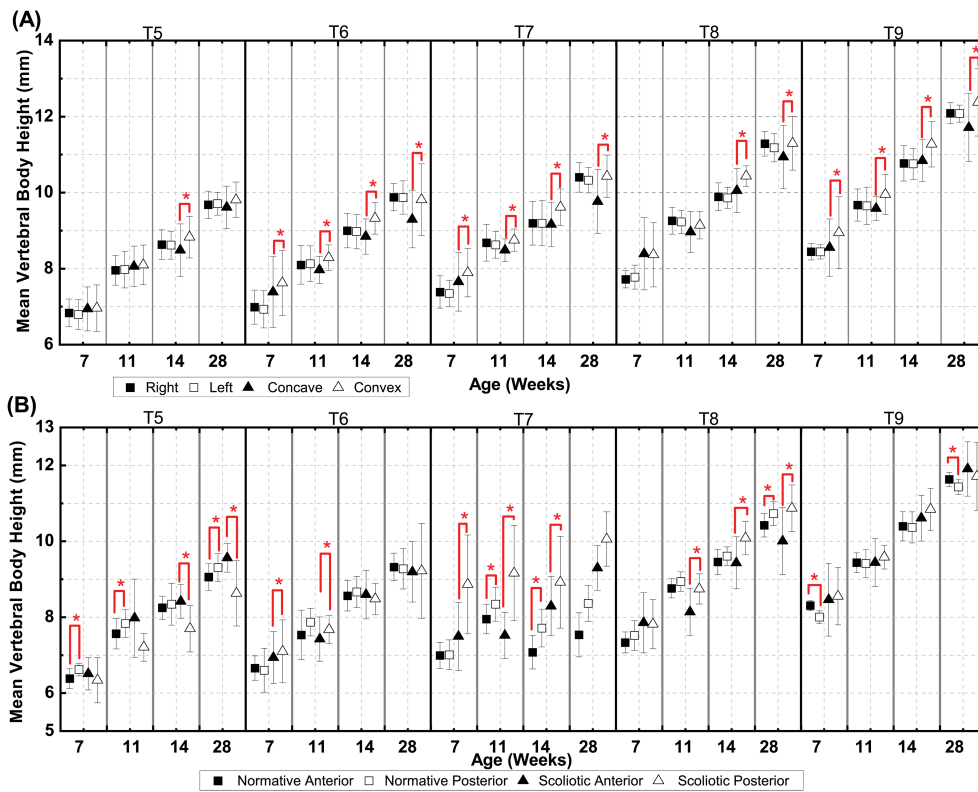


FIGURE 5 Mean and SD of thoracic vertebral body height for normative and scoliotic groups, (A) Right and Left, and Concave and Convex, (B) Anterior and Posterior

2.5 | Relationships between vertebral wedging, spine curvature, and moment-arm of rib tether

In order to predict the extent of vertebral wedging that would result from a progressive spine deformity, two linear regression models were created: (1) sum of vertebral wedging in the frontal and sagittal planes i.e., $(VB_{CX}^H / VB_{CC}^H) + (VB_P^H / VB_A^H)$ versus the sum of moment-arms in the frontal and sagittal planes (i.e., $a + b$), and (2) sum of moment-arms in the frontal and sagittal planes (i.e., $a + b$) versus the sum of Cobb and kyphosis angles.

3 | RESULTS

3.1 | Vertebral body heights

For both normative and scoliotic groups, VBH (VB_L^H , VB_R^H , VB_{CX}^H , VB_{CC}^H , VB_P^H , VB_A^H), increased with age and with increasing thoracic levels (i.e., from T5 to T9). Comparisons between the normative and scoliotic right, left, anterior and posterior VBH at time points 7, 11, 14, and 28 weeks are shown in Figure 5. However, no significant differences were found between normal and scoliotic groups.

3.2 | Bilateral and Anterior-Posterior symmetry

In the normative group, no significant differences were observed between VB_R^H and VB_L^H at each level and at any time point. However, in the scoliotic group, significant differences were found between

VB_{CC}^H and VB_{CX}^H (Figure 5A) at T6, T7, and T9 at all time points, at T5 at 14 weeks, and at T8 at 14 and 28 weeks. For both groups, significant differences (i.e., A-P asymmetry) were found between VB_A^H and VB_P^H at several levels, with greater differences observed in the scoliotic group (Figure 5B).

3.3 | Vertebral wedging

The ratio of bilateral VBH were found to be significantly different between normative VB_L^H / VB_R^H and scoliotic (VB_{CX}^H / VB_{CC}^H) groups at T5 (14 and 28 weeks), T6 and T7 at (7-14 weeks), and T8 and T9 at (14 weeks). Between normative and scoliotic groups, significant differences were observed in VB_P^H / VB_A^H at T5 at all-time points and at T7 at time of 7 weeks (Figure 6).

3.4 | Growth rates

An exemplar scatter plot with T7 convex vertebral body height and regression line is shown in Figure 7. The vertebral body growth rate (i.e., coefficient of the linear regression model) for T5-T9 are shown in Table 3. The overall average growth rate for vertebral body height in the normative group was 0.0182 mm/day, and scoliotic group was 0.0163 mm/day. No statistically significant differences were found in the vertebral body growth rates between normative and scoliotic groups, and no significant differences were found across vertebral levels for the normative and scoliotic groups.

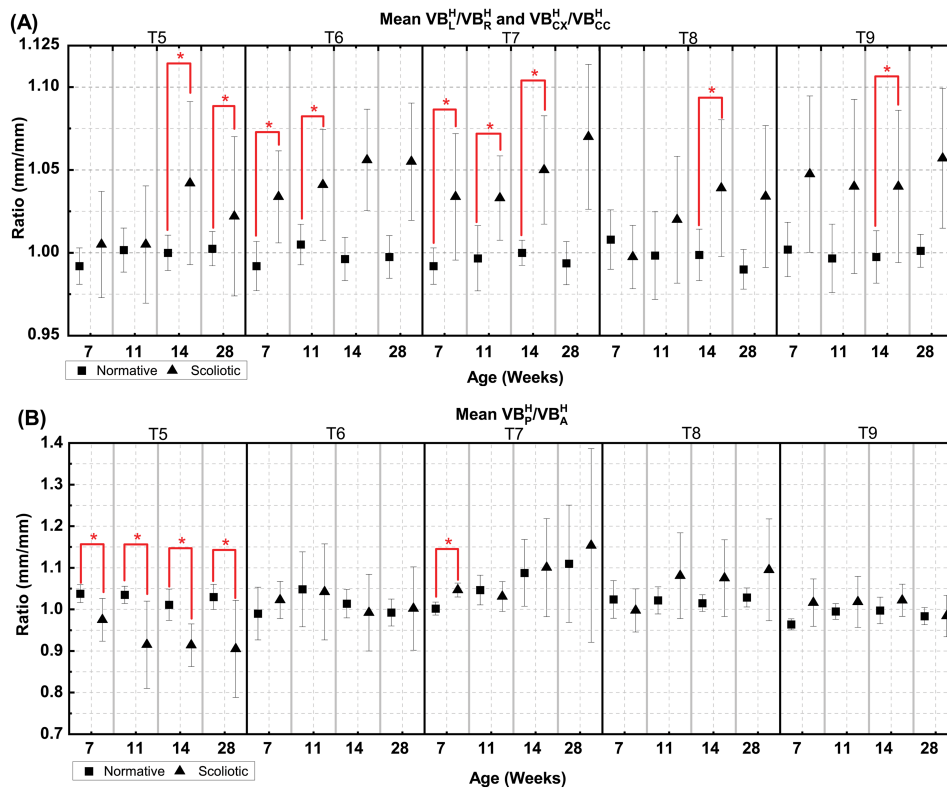


FIGURE 6 Mean and SD of thoracic vertebral body height ratio for normative and scoliotic groups, (A) VB_L^H/VB_R^H and VB_{CX}^H/VB_{CC}^H (B) VB_P^H/VB_A^H

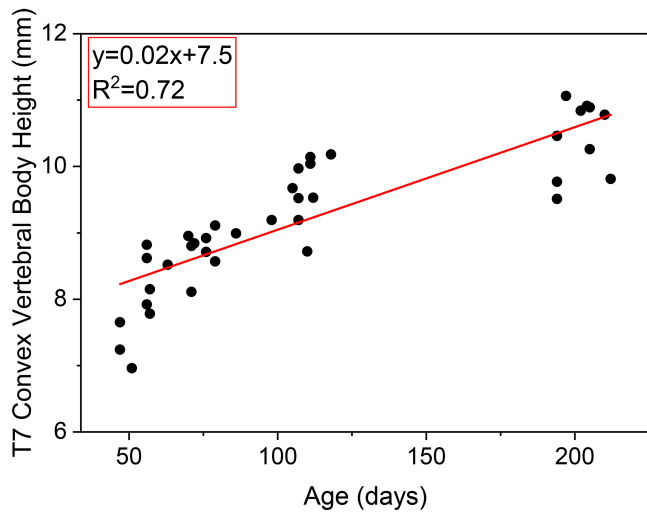


FIGURE 7 Scatter plot showing T7 convex vertebral body height as a function of age and the respective linear regression line. The coefficient of the linear regression model represents the rate of change for the measurement (mm/day)

3.5 | Relationships between vertebral wedging, spine curvature, and moment-arm of rib tether

The sum of vertebral wedging at the apical level (T7) in the frontal and sagittal planes positively and significantly ($p < .01$) correlated

to the sum of the moment-arms for T3-T9 (Figure 8A). Additionally, the sum of the moment-arms for T3-T9 positively and significantly correlated ($p < .001$) with the sum of the Cobb angle and the Kyphosis angle (Figure 8B).

3.6 | Spine curvature

Based on previously published data from this study, the magnitude of the spine curvature at 7 weeks, as measured by maximum deformity angle (MDA), highly correlated ($R^2 = 0.89$) with the MDA at 28 weeks.²² Since MDA cannot be easily measured from radiographs, the sum of the Cobb and kyphosis angles was used as a measure of spine deformity. The sum of the Cobb and kyphosis angles at 7 weeks also highly correlated ($R^2 = 0.92$) with the sum of the Cobb and kyphosis angles at 28 weeks (Figure 9).

4 | DISCUSSION

The current study provides novel data on longitudinal growth patterns of the thoracic vertebrae in normative and scoliotic rabbits. In both normative and scoliotic groups, thoracic VBH increased with increasing age and increasing vertebral level. This may be indicative of structural adaptations to increasing axial and

TABLE 3 Coefficients from linear regression models

| Measurement (mm) | Group | T5 | T6 | T7 | T8 | T9 |
|------------------|-----------|----------|----------|----------|----------|----------|
| VB_R^H | Normative | 6.5037 | 6.6947 | 7.0329 | 7.3363 | 7.9257 |
| | | [0.0166] | [0.0169] | [0.0176] | [0.0206] | [0.0218] |
| | | <0.8049> | <0.7622> | <0.7839> | <0.8564> | <0.8478> |
| VB_{CC}^H | Scoliotic | 6.6080 | 7.0793 | 7.4125 | 7.8105 | 8.1260 |
| | | [0.0154] | [0.0120] | [0.0126] | [0.0163] | [0.0190] |
| | | <0.6555> | <0.5151> | <0.5348> | <0.6139> | <0.6600> |
| VB_L^H | Normative | 6.4634 | 6.6657 | 7.0288 | 7.4119 | 7.9073 |
| | | [0.0170] | [0.0171] | [0.0173] | [0.0196] | [0.0218] |
| | | <0.8062> | <0.7522> | <0.7912> | <0.8508> | <0.8543> |
| VB_{CX}^H | Scoliotic | 6.6466 | 7.2774 | 7.5009 | 7.7960 | 8.3645 |
| | | [0.0165] | [0.0137] | [0.0155] | [0.0186] | [0.0210] |
| | | <0.6917> | <0.5498> | <0.7206> | <0.7320> | <0.6759> |
| VB_A^H | Normative | 6.2166 | 6.3352 | 6.5091 | 7.1612 | 7.8251 |
| | | [0.0151] | [0.0159] | [0.0167] | [0.0173] | [0.0198] |
| | | <0.7597> | <0.7329> | <0.8102> | <0.7918> | <0.8698> |
| | Scoliotic | 6.2855 | 6.4321 | 6.7638 | 7.3059 | 7.7985 |
| | | [0.0170] | [0.0148] | [0.0114] | [0.0143] | [0.0213] |
| | | <0.6359> | <0.5946> | <0.4118> | <0.5143> | <0.7100> |
| VB_P^H | Normative | 6.3945 | 6.5393 | 6.7788 | 7.2546 | 7.7241 |
| | | [0.0153] | [0.0148] | [0.0166] | [0.0182] | [0.0196] |
| | | <0.7580> | <0.6586> | <0.7462> | <0.8263> | <0.8087> |
| | Scoliotic | 6.0120 | 6.6585 | 7.1378 | 7.3286 | 8.1260 |
| | | [0.0135] | [0.0135] | [0.0155] | [0.0190] | [0.0190] |
| | | <0.5834> | <0.4950> | <0.6615> | <0.7399> | <0.6600> |

Note: The linear regression model is given by the equation: geometric measure (in mm) = $b_1 \cdot (\text{age in days}) + b_0$. Coefficient b_0 , the approximate parameter value at birth is the value in the first row, Coefficient b_1 is the increase in parameter value per day, shown in the second row ([]); and R^2 (Percentage of variance explained by the model is the value in the third row (<>).

Abbreviations: VBH, vertebral body heights.

compressive loading caused by muscle forces and body weight, respectively. While bilateral (right-left) symmetry was observed in the normative group, bilateral asymmetry was observed between the convex (left) and concave (right) sides in the scoliotic group, with reduced heights on the concave side. However, there were no significant differences in the dimensions between the normative and scoliotic vertebrae. In both groups, there was asymmetry between the posterior and anterior VBH, with relatively greater posterior vertebral body height. Also, the A-P asymmetry was greater in the scoliotic vertebrae as compared to the normative group. It is interesting to note that the anteriorly directed wedging (A-P asymmetry) was similar to that observed in normative pediatric human thoracic vertebrae.²⁴

The morphological bilateral and A-P asymmetries observed in the scoliotic vertebrae are similar to those previously reported in immature scoliotic porcine and bovine spine.²⁷⁻³⁰ In the scoliotic group, the asymmetric growth in T6 and apical level (T7) in the coronal plane and at T7 and T8 in the sagittal plane could be a result of varying load patterns associated with curve progression.

These findings may corroborate the vicious cycle theory proposed by Stokes et al (1996)¹⁶ which hypothesized that asymmetric vertebral growth patterns are initiated by asymmetric loading. Also, the multi-planar vertebral wedging seen in the scoliotic rabbits was similar to the typical three-dimensional vertebral deformity in scoliotic humans.³¹ Despite significant lateral curvature and vertebral wedging in scoliotic rabbits, only a few significant differences were found in VBH between normative and scoliotic vertebrae. The overall spine deformity may also be due to changes in disc shape. Will et al (2009) showed that initial deformity early in the growth spurt happens in the IVD whereas vertebral wedging was noticed after the peak height velocity (PHV).³ Moreover, Upasani et al (2011) reported disc wedging toward the tether in immature Yucatan mini-pigs with anterior spinal instrumentation.³⁰

While there were significant differences in vertebral morphology between normative and scoliotic rabbits, there were no differences in vertebral body growth rates between these two groups. However, in scoliotic vertebrae, VB_{CX}^H and VB_P^H showed higher

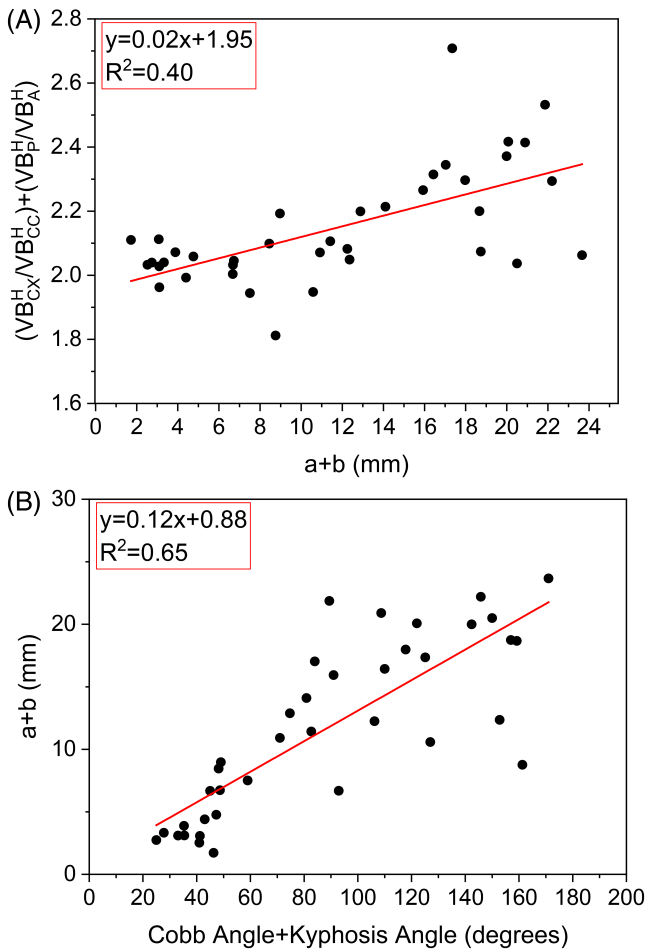


FIGURE 8 (A) Correlation between the sum of vertebral body wedging and the sum of their corresponding moment-arms at the apical level (T7) (B) Correlation between the sum of moment-arms and the sum of their corresponding Cobb angle and kyphosis angle at the apical level (T7)

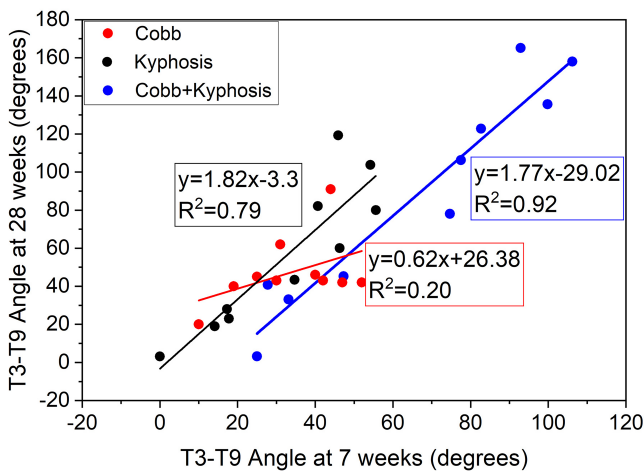


FIGURE 9 Linear regression between Cobb angle at 7 weeks and 28 weeks, Kyphosis angle at 7 weeks and 28 weeks, and the sum of the kyphosis and Cobb angles at 7 weeks and 28 weeks

growth rates than VB_{CC}^H and VB_A^H , respectively. These growth patterns support Heuter-Volkman principle which states that compressive loads inhibit growth while tensile loads promote growth.³² The average growth rates at T5-T9 levels for normative rabbits were 0.019 mm/day (left-right) and 0.017 mm/day (Anterior-Posterior), respectively. These normative values were greater than the average T5-T9 scoliotic growth rates of 0.015 mm/day (for VB_{CC}^H) and 0.017 mm/day (for VB_{CX}^H), as well as for VB_A^H (0.015 mm/day) and VB_P^H (0.013 mm/day). These results indicate that the compressive forces acting on the scoliotic vertebral bodies may be greater than those on the normative spine. Also, there may be more compressive forces acting on the concave side as compared to the convex side. As compared to vertebral body growth in humans, the growth rates in normative rabbits were approximately seven times higher.²⁴ Continuous increase in longitudinal growth on the convex side of a curve and inhibition on the concave side results in vertebral wedging which is a key structural characteristic of progressive spine deformity.^{8,33}

Recent studies by Wren et al (2017)³⁴ and Poorghasamians et al (2017)³⁵ reported that a smaller vertebral cross-sectional area was associated with lesser strength and greater flexibility (i.e., greater range of motion). Also, smaller vertebrae have greater magnitude of asymmetric vertebral loading due to increase in flexibility, which in turn leads to progression of vertebral wedging. As vertebral geometry is a likely determinant of the extent of vertebral wedging, it is important to decouple the effects of geometry to better understand the interplay between vertebral wedging and spine curvature. Hence, we examined the effects of the moment-arm of the rib tether, which is a proxy for the applied tether force, with vertebral wedging and spine curvature. Our results showed that both vertebral wedging and spine curvature positively correlated with the moment-arm of the rib tether. Growth modulation procedures to correct spine deformity could use such relationships to predict the amount of vertebral wedging or spine curvature that would result from an asymmetric corrective force, measured as a moment-arm.

A major limitation of this study is its retrospective nature. Because it is retrospective, scans at some time points were not available for all rabbits for analysis. However, 13 out of 18 rabbits had four time points and three rabbits had three time points and two rabbits had two time points. In addition, The rib-tethering surgery was unevenly effective in creating thoracic deformity, in particular, in the case of ribs fracture occurrence during the tethering procedure, it leads to a reduced moment on the thoracic spine lessening the deformity. However, all rabbits included in this study successfully developed a progressive deformity. Although there may be differences in magnitude and mode of loading between quadruped and biped spines, the results from this study provides valuable insight on the effects of asymmetric loading on vertebral growth. While the current results cannot be directly extrapolated to human vertebral growth due to anatomical differences and inter-species differences in rate of skeletal maturation, similar data gathered from humans can be used to inform the timing and vertebral levels selection for vertebral growth

modulation. Future studies could focus on studying the relationship between applied stress and resulting growth.

CONFLICT OF INTEREST

The authors declare no potential conflict of interest.

AUTHORS CONTRIBUTION

Ausilah Alfraitat: Methodology, software, formal analysis, investigation, writing - original draft, visualization.

John Casey Olson: Methodology, resources, data curation, writing - review and editing.

Brian D. Snyder: Methodology, resources, formal analysis, writing - review and editing.

Patrick J. Cahill: Formal analysis, writing - Review and Editing.

Sriram Balasubramanian: Conceptualization, methodology, formal analysis, resources, data curation, writing - original draft, visualization, Supervision, Project administration, funding acquisition.

ORCID

Ausilah Alfraitat  <https://orcid.org/0000-0003-2255-0081>

REFERENCES

- Illés TS, Lavaste F, Dubouset JF. The third dimension of scoliosis: The forgotten axial plane. *Orthopaedics & Traumatology: Surgery & Research*. 2019;105(2):351-359. <https://doi.org/10.1016/j.otsr.2018.10.021>.
- National Scoliosis Foundation. *Information and Support*. 2019.
- Will RE, Stokes IA, Qiu X, Walker MR, Sanders JO. Cobb angle progression in adolescent scoliosis begins at the intervertebral disc. *Spine*. 2009;34(25):2782-2786. <https://doi.org/10.1097/brs.0b013e3181c11853>
- Schlösser Tom PC, van Stralen M, Brink RC, Chu Winnie CW, Lam T-P, Vincken KL, Castelein RM, Cheng Jack CY. Three-dimensional characterization of torsion and asymmetry of the intervertebral discs versus vertebral bodies in adolescent idiopathic scoliosis. *Spine*. 2014;39(19):E1159-E1166. <https://doi.org/10.1097/brs.0000000000000467>.
- Veldhuizen A, Wever D, Webb P. The aetiology of idiopathic scoliosis: biomechanical and neuromuscular factors. *Eur Spine J*. 2000;9:178-184.
- Stokes IA. Analysis of symmetry of vertebral body loading consequent to lateral spinal curvature. *Spine*. 1997;22:2495-2503.
- Villemure I, Aubina CE, Dansereau J, Labelle H. Simulation of progressive deformities in adolescent idiopathic scoliosis using a biomechanical model integrating vertebral growth modulation. *J Biomech Eng*. 2002;124:784-790.
- Mente PL, Spence H, Aronsson DD. Progression of vertebral wedging in an asymmetrically loaded rat tail model. *Spine*. 1997;22:1292-1296.
- Andriacchi TP, Schultz AB, Belytschko T, Dewald R. Milwaukee brace correction of idiopathic scoliosis. A biomechanical analysis and a retrospective study. *J Bone Joint Surg Am*. 1976;58:806-815.
- Périé D, Aubin C-E, Petit Y, Beauséjour M, Dansereau J, Labelle H. Boston brace correction in idiopathic scoliosis: a biomechanical study. *Spine*. 2003;28:1672-1677.
- Vitale MG, Matsumoto H, Roye DP, Gomez JA, Betz RR, Emans JB, Skaggs DL, Smith JT, Song KM, Campbell RM. Health-related quality of life in children with thoracic insufficiency syndrome. *Journal of Pediatric Orthopaedics*. 2008;28(2):239-243. <https://doi.org/10.1097/bpo.0b013e31816521bb>.
- Vitale MG, Matsumoto H, Bye MR, Gomez JA, Booker WA, Hyman JE, Roye DP. A retrospective cohort study of pulmonary function, radiographic measures, and quality of life in children with congenital scoliosis. *Spine*. 2008;33(11):1242-1249. <https://doi.org/10.1097/brs.0b013e3181714536>.
- Jain V, Lykissas M, Trobisch P, et al. Surgical aspects of spinal growth modulation in scoliosis correction. *Instr Course Lect*. 2014;63:335-344.
- Crawford CH III, Lenke LG. Growth modulation by means of anterior tethering resulting in progressive correction of juvenile idiopathic scoliosis: a case report. *JBJS*. 2010;92:202-209.
- Newton PO, Kluck DG, Saito W, Yaszay B, Bartley CE, Bastrom TP. Anterior spinal growth tethering for skeletally immature patients with scoliosis: a retrospective look two to four years postoperatively. *JBJS*. 2018;100:1691-1697.
- Stokes IA, Spence H, Aronsson DD, Kilmer N. Mechanical modulation of vertebral body growth: implications for scoliosis progression. *Spine*. 1996;21:1162-1167.
- Aronsson DD, Stokes I, Rosovsky J, Spence H. Mechanical modulation of calf tail vertebral growth: implications for scoliosis progression. *J Spinal Disord*. 1999;12:141-146.
- Stokes IA, Aronsson DD, Dimock AN, Cortright V, Beck S. Endochondral growth in growth plates of three species at two anatomical locations modulated by mechanical compression and tension. *J Orthop Res*. 2006;24:1327-1334.
- Buttermann GR, Beaubien BP, Saeger LC. Mature runt cow lumbar intradiscal pressures and motion segment biomechanics. *Spine J*. 2009;9:105-114.
- Reitmaier S, Schmidt H, Ihler R, et al. Preliminary investigations on intradiscal pressures during daily activities: an in vivo study using the merino sheep. *PLoS One*. 2013;8:e69610.
- Smit TH. The use of a quadruped as an in vivo model for the study of the spine—biomechanical considerations. *Eur Spine J*. 2002;11:137-144.
- Olson JC, Takahashi A, Glotzbecker MP, Snyder BD. Extent of spine deformity predicts lung growth and function in rabbit model of early onset scoliosis. *PLoS One*. 2015;10:e0136941.
- Olson JC. *Quantitative Pathophysiology in a Rabbit Models of Early Onset Scoliosis and Expansion Thoracoplasty*. Boston, MA: Boston University; 2014. <https://hdl.handle.net/2144/11160>.
- Peters JR, Chandrasekaran C, Robinson LF, Servaes SE, Campbell RM Jr, Balasubramanian S. Age- and gender-related changes in pediatric thoracic vertebral morphology. *Spine J*. 2015;15:1000-1020.
- Peters JR, Campbell RM, Balasubramanian S. Characterization of the age-dependent shape of the pediatric thoracic spine and vertebrae using generalized procrustes analysis. *J Biomech*. 2017;63:32-40.
- Balasubramanian S, Peters JR, Robinson LF, Singh A, Kent RW. Thoracic spine morphology of a pseudo-biped animal model (kangaroo) and comparisons with human and quadruped animals. *European Spine Journal*. 2016;25(12):4140-4154. <https://doi.org/10.1007/s00586-016-4776-x>.
- Braun JT, Hoffman M, Akyuz E, Ogilvie JW, Brodke DS, Bachus KN. Mechanical modulation of vertebral growth in the fusionless treatment of progressive scoliosis in an experimental model. *Spine*. 2006;31:1314-1320.
- Newton PO, Faro FD, Farnsworth CL, et al. Multilevel spinal growth modulation with an anterolateral flexible tether in an immature bovine model. *Spine*. 2005;30:2608-2613.
- Newton PO, Upasani VV, Farnsworth CL, et al. Spinal growth modulation with use of a tether in an immature porcine model. *JBJS*. 2008;90:2695-2706.
- Upasani VV, Farnsworth CL, Chambers RC, et al. Intervertebral disc health preservation after six months of spinal growth modulation. *J Bone Joint Surg Am*. 2011;93:1408-1416.

31. Parent S, Labelle H, Skalli W, Latimer B, de Guise J. Morphometric analysis of anatomic scoliotic specimens. *Spine*. 2002;27:2305-2311.
32. Mehlman CT, Araghi A, Roy DR. Hyphenated history: the Hueter-Volkman law. *Am J Orthoped-belle Mead*. 1997;26:798-800.
33. Mente PL, Aronsson DD, Stokes IA, Iatridis JC. Mechanical modulation of growth for the correction of vertebral wedge deformities. *J Orthop Res*. 1999;17:518-524.
34. Wren TA, Ponrartana S, Aggabao PC, Poorghasamians E, Gilsanz V. Association between vertebral cross-sectional area and vertebral wedging in children and adolescents: a cross-sectional analysis. *J Bone Miner Res*. 2017;32:2257-2262.
35. Poorghasamians E, Aggabao PC, Wren TA, Ponrartana S, Gilsanz V. Vertebral cross-sectional growth: a predictor of vertebral wedging in the immature skeleton. *PLoS One*. 2017;12:e0190225.

How to cite this article: Alfraih A, Olson JC, Snyder BD, Cahill PJ, Balasubramanian S. Thoracic vertebral morphology in normal and scoliosis deformity in skeletally immature rabbits: A Longitudinal study. *JOR Spine*. 2020;3:e1118.
<https://doi.org/10.1002/jsp2.1118>